



## The transition from tortuous to rectilinear cosmic ray trajectories in the Galaxy is at the origin of the knee and the ankle

A. CODINO<sup>1</sup>, F. PLOUIN<sup>2</sup>.

<sup>1</sup>*INFN and Dip. di Fisica dell'Università degli Studi di Perugia, Via A. Pascoli, 06123 Perugia, Italy*

<sup>2</sup>*Former CNRS researcher, Ecole Polytechnique, LLR, F-91128 Palaiseau, France*

*antonio.codino@pg.infn.it*

**Abstract:** The shapes of cosmic ray trajectories in the Galaxy result from the effect of a chaotic and regular magnetic field, the rates of the nuclear collisions, the gas density and other minor parameters. For a given magnetic field configuration the forms of the trajectories, regardless their lengths, naturally subdivide in rectilinear and highly tortuous, depending on the ion energy. It is shown that the ankle and the knee energies of the individual ions correspond to those particular energies of the ion traversing the Milky Way which mark, respectively, the rectilinear and the tortuous propagation. A comparison with the computed proton, helium, CNO, iron and all-particle spectrum with the experimental data is presented and the good accord highlighted.

### Introduction

Radioastronomy in the last three decades redundantly proved that spiral galaxies possess a regular magnetic field, with a strength not exceeding  $10 \mu\text{G}$ , extending over the Galaxy, along with a turbulent field with superior strength. These features result from observations and they are likely to stabilize with any future measurements with increased precision. The size of the Galaxy and the density of the interstellar gas are well known from Astronomy.

These observations, the nuclear collision lengths and simple formulae giving the quantitative bending of electric charges moving in magnetic fields, suffice to demonstrate the existence and the nature of the knee and the ankle in the cosmic ray spectrum.

In the following, a derivation of some properties of the knee and ankle is given with short flashes on its simplicity and logical coherence. This derivation follows a very detailed explanation of the knee and ankle [1, 2, 3], (also referred to as Paper I, II and III) the description of the method of calculation [4, 5] and the notion of the galactic basin [5, 6].

The comprehension of the mechanisms originating the ankle and the knee is greatly facilitated if the

logical chain connecting the pertinent facts is examined at very high energy, around the ankle energy and not at very low energy, below the knee. At very high energy, neither the magnetic field nor nuclear cross sections have a notable influence on the properties of the cosmic rays and any analysis simplifies.

### What is a cosmic ray trajectory

Figures 1 and 2 show an iron and a helium trajectory at the energy of  $10^{18}$  and  $10^{12}$  eV, respectively. A trajectory consists of an initial point (the source represented by a star) and of a final point (cross) connected by thousands of segments (representing helix segments at high energy or helix axis at very low energy). Trajectories are reconstructed by numerical simulation and are temporarily stored during the simulation for the evaluation of the appropriate physical quantities.

The visual inspection of the forms of the trajectories in the energy interval  $10^{11}$  to  $10^{20}$  eV naturally suggests three major classes of trajectories: *R*, *T* and *M*. (*R*) The magnetic field has a negligible effect on the trajectory so that rectilinear or quasi rectilinear propagation takes place above

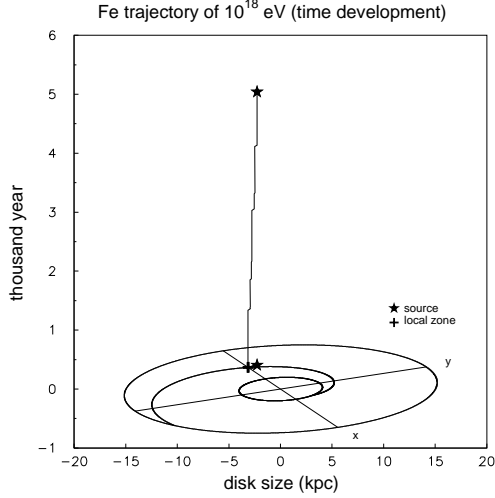


Figure 1: Example of iron trajectory of  $10^{18}$  eV propagating in the disc for about 5000 years (vertical axis). It is evident that this Fe trajectory is only slightly perturbed by the chaotic magnetic field. This trajectory strikingly differs from the highly tortuous trajectory shown in figure 2.

a particular energy  $E_A^g$  where  $A$  denotes the ion type and  $g$  galactic cosmic rays. All trajectories at energies above  $E_A^g$  are quite similar. Detailed calculations indicate  $E_{He}^g = 4 \times 10^{18}$  eV and  $E_{Fe}^g$  around  $6 \times 10^{19}$  eV. (T) Cosmic ions suffering multiple inversions of motion in the magnetic field lead to tortuous or very tortuous trajectories as shown in figure 2. (M) The ion bending operated by the galactic magnetic field consists of a few turns around the helix axis of the cosmic ion (see fig. 4 Paper III). Detailed analysis of many ion trajectories indicates that the energy interval where trajectories exhibit these forms is between  $10^{15}$  and  $6 \times 10^{19}$  eV because of the average magnetic field strength in the Milky Way. The Fe trajectory of  $10^{18}$  eV in figure 1 illustrates this condition. Though there is an infinite number of ways how cosmic rays become tortuous, depending on the turbulent field incorporated in the algorithms, the mean trajectory lengths in the Galaxy remain finite.

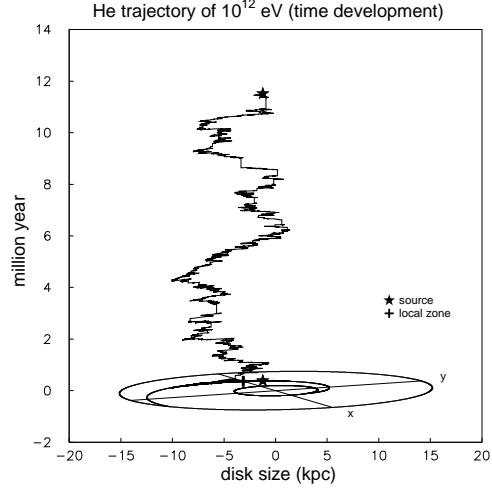


Figure 2: Example of helium trajectory at very low energy (1 TeV).

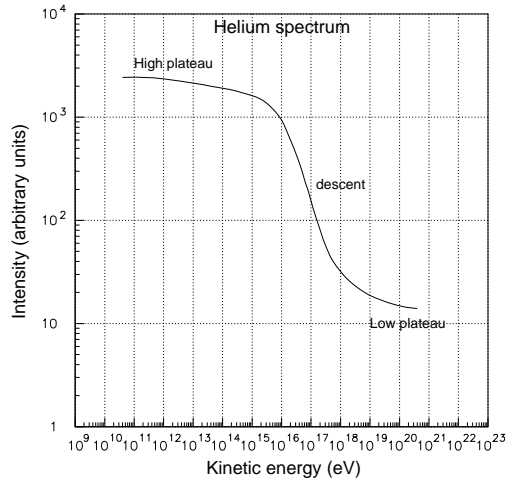


Figure 3: Number of cosmic rays (He) reaching the local galactic zone,  $n_g$ , versus energy. This quantity is related to helium intensity via the spectral index of cosmic helium at Earth. The structure of the curve exhibits a high plateau, a steep descent and a low plateau.

## Evaluation of the cosmic ray intensities

The parameters that determine the cosmic-ray intensity are the following: (1) the spiral magnetic field; (2) the strength of the spiral magnetic field (fig. 3, Paper III); (3) the chaotic magnetic field, materialized with magnetic cloudlets, which has an average strength of about three times that of the regular field; (4) the form and the dimension of the Galaxy (fig. 1 [4]); (5) a uniform distribution of cosmic ray sources in the galactic disk (see eqn.(3) in [4]); (6) the nuclear cross sections ion-hydrogen,  $\sigma$ ; (7) the interstellar matter density in the disk,  $d$ , of 1.24 hydrogen atoms per  $cm^3$ ; (8) the position of the *solar cavity* inside the disk, at 14  $pc$  above the galactic midplane and 8.5  $kpc$  from the galactic center; (9) the galactic wind (Section 2, Paper III). The present calculations are obtained ignoring the galactic wind since its influence on the knee and ankle is marginal (figs. 17 and 18, Paper III).

The intensity of the cosmic rays,  $I_P$ , in a given point  $P$  of coordinates  $x,y,z$  inside the galactic disc is evaluated by counting the number of trajectories,  $n_g$ , intercepting a small sphere centered in  $P$ . Figure 3 shows  $n_g$  versus energy for helium taken as an example. The realm of the tortuous trajectories spans the energy domain labeled in figure 3 as high plateau, while rectilinear trajectories occupy the energy band denoted as low plateau. The differences between low and high plateaux is due to the ion grammages and nuclear cross sections as explained elsewhere (Section 7, Paper II) and they determine the slope of the *complete spectrum* above  $6 \times 10^{15}$   $eV$ . In order to convert  $n_g$  into  $I_P$  the spectral index of helium should be taken into account. Figure 4 shows the ion intensities  $I_P$  for a set of six spectral indices. Comparing the helium spectrum shown in figure 4 with  $n_g$  versus energy of figure 3 it is evident how the low plateau is converted into the helium ankle with its intrinsic characteristics.

Computed and measured spectra of proton, helium, CNO group and iron are displayed in figure 5. Figure 6 shows the computed and measured spectrum of all ions using the blend 2 (Table 2, Paper II). The knee and the ankle are local effects: a terrestrial instrument encapsulated at 8.5  $kpc$  from the galactic center, close to the galactic midplane, will observe the knee and the ankle, while another instrument

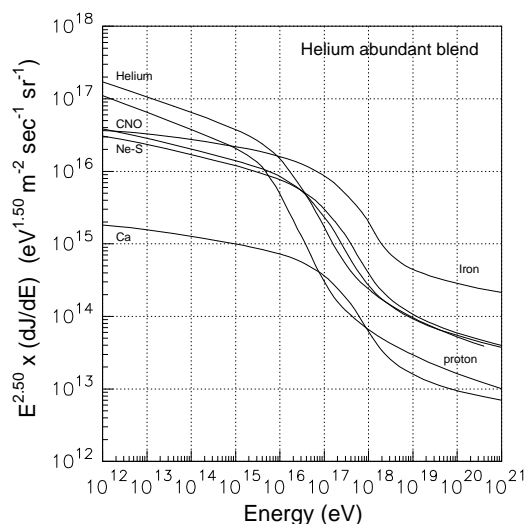


Figure 4: Examples of energy spectra of individual ions for a specified set of spectral indices and ion abundances (blend 2, Table 1, Paper II).

located 100  $pc$  above the galactic midplane at the same distance, would observe and anti-knee (fig. 17, Paper II) and an anti-ankle.

Analytical methods with appropriate magnetic field in the diffusion equation (see, for example, [7]) predict a type of descend similar to that shown in figure 3 but the interconnection between knee and ankle and how the nuclear cross sections determine the gap between high and low plateau (Section 9, Paper I) are eluded. Plausibly, numerical simulation of cosmic-ion trajectories at extreme energies (see, for example, [8]), once extended to lower energies down to  $10^{14}$   $eV$ , may verify the present explanation of the knee and the ankle.

Nuclear collision lengths spanning from 55 (proton) to 2 (iron)  $g/cm^2$  overlap the ranges of the grammages of cosmic ions traversing the Milky Way, probably a *lusus naturae*. This circumstance transforms the nuclear collision rates in the Milky Way in a major parameter for a quantitative account of the knee and the ankle. In dwarf galaxies, where the ion grammages are likely to be marginal fractions of those experienced by cosmic ions in the Milky Way, the knees and the ankles should not exist at all, leaving the universal spec-

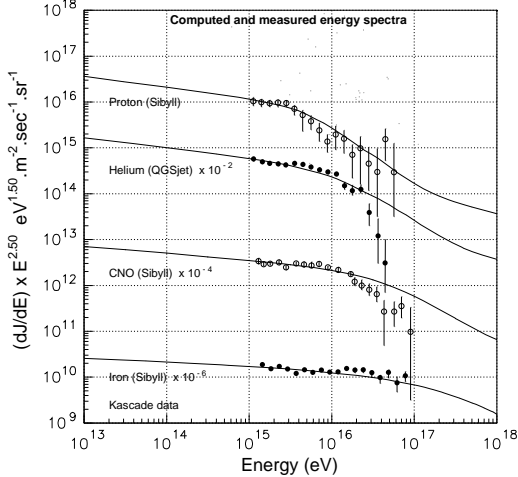


Figure 5: The computed spectra (thick lines) are compared with the Cascade data for proton, He, CNO [9] and Fe [10]. All spectra are normalized at the common energy point of  $2 \times 10^{15}$  eV to the proton, helium, CNO and iron and they are computed with indices: 2.72 (proton), 2.72 (He) and 2.60 (CNO and Fe).

trum of the cosmic radiation in its unperturbed status, as directly released by the engine accelerating cosmic ions at all energies.

## References

- [1] A. Codino, F. Plouin, Nucl. Phys. B, (Proc. Suppl.) 165 (2007) 307–316.
- [2] A. Codino, F. Plouin, Proc. VULCANO Conf. 2006 and Astro-ph/0701521, Jan. 18th.
- [3] A. Codino, F. Plouin, Galactic basins of helium and iron around the knee energy, INFN Report, INFN/TC-06/05, Frascati, Italy and Astro-ph/0701498, Jan. 17th.
- [4] M. Brunetti, A. Codino, Astrophys. Jour. 528 (2000) 789–798.
- [5] A. Codino, F. Plouin, Astrophys. Jour. 639 (2006) 173–184.
- [6] A. Codino, F. Plouin, Proc. 28th ICRC, Tsukuba, Japan III (2003) 173.

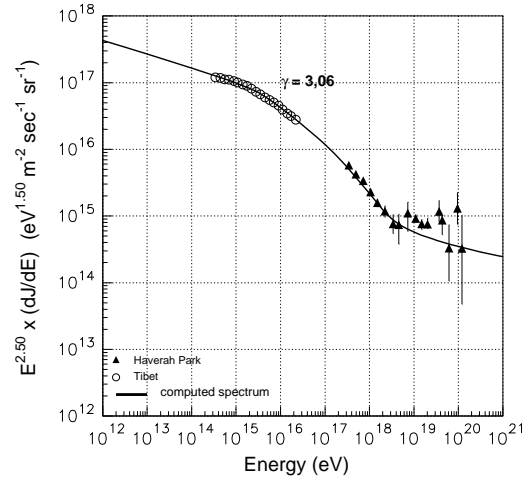


Figure 6: The computed spectrum (thick line) is compared with the data of Akeno [11] and Haverah Park [12] experiments showing an excellent agreement in the full band  $4 \times 10^{14} - 10^{20}$  eV. Note that only one energy point ( $10^{16}$  eV) is used in the normalization of the computed spectrum to the data.

- [7] G. Candia, E. Roulet, L. Epele, Journal of High Energy Physics 12 (2002) 33.
- [8] R. Lampard, R. Clay, B. Dawson, Astropart. Phys. 7 (1997) 213–218.
- [9] T. Antoni, al. (Kascade Coll.), Astropart. Phys. 24 (2005) 1–25.
- [10] M. Roth, al., Proc. 28th ICRC, Tsukuba, Japan V (2003) 305.
- [11] M. Amenomori, al. (Tibet Coll.), Astrophys. Jour. 461 (1996) 408.
- [12] M. Lawrence, al. (Haverah Park Coll.), Proc. 21th ICRC, Adelaide, Australia 3 (1990). Ave, M. et al., Astro-ph/0112253 (data revision), 2002) 159.